Localization properties of groups of eigenstates in chaotic systems

D. A. Wisniacki,[1,2] F. Borondo,[1] E. Vergini,[2] and R. M. Benito[3]
[1]*Departamento de Química C–IX, Universidad Autónoma de Madrid, Cantoblanco, E28049 Madrid, Spain*
[2]*Departamento de Física, Comisión Nacional de Energía Atómica, Avenida del Libertador 8250, 1429 Buenos Aires, Argentina*
[3]*Departamento de Física y Mecánica, Escuela Técnica Superior de Ingenieros de Telecommunicación Agrónomos, Universidad Politécnica de Madrid, E28009 Madrid, Spain*
(Received 18 December 2000; published 29 May 2001)

In this paper we study in detail the localized wave functions defined in Phys. Rev. Lett. **76**, 1613 (1994), in connection with the scarring effect of unstable periodic orbits in highly chaotic Hamiltonian system. These functions appear highly localized not only along periodic orbits but also on the associated manifolds. Moreover, they show in phase space the hyperbolic structure in the vicinity of the orbit, something that translates in configuration space into the structure induced by the corresponding self-focal points. On the other hand, the quantum dynamics of these functions are also studied. Our results indicate that the probability density first evolves along the unstable manifold emanating from the periodic orbit, and localizes temporarily afterwards on only a few, short related periodic orbits. We believe that this type of study can provide some keys to disentangle the complexity associated with the quantum mechanics of these kind of systems, which permits the construction of a simple explanation in terms of the dynamics of a few classical structures.

DOI: 10.1103/PhysRevE.63.066220 PACS number(s): 05.45.−a, 05.45.Mt, 03.65.Sq

I. INTRODUCTION

The investigation of the quantum manifestations of classical chaos is at present a very active field of research [1]. The relationship between quantum dynamics and classical invariants, mainly periodic orbits (PO) and their associated manifolds, is not satisfactorily understood yet [2]. In this respect, an important achievement would be to disentangle the time evolution of a quantum system whose classical analog is chaotic, explaining this dynamics in terms of classical structures.

Fifteen years ago, a seminal step was done by Heller [3], who considered the evolution of a wave packet localized on an unstable PO. He found that the dynamics in the short-time limit are controlled by the motion around the orbit and its Lyapunov exponent and is well understood in terms of semiclassical expressions [3,4].

For longer times the dynamical mixing induced by the chaotic behavior of the motion makes the situation more complicated, and one single orbit and the linearized dynamics around it is not enough to account for the evolution of the wave packet. Some time later, Tomsovic and Heller [5] showed that even for those long times, for which classical fine structure had developed on a scale much smaller than $\hbar$, the semiclassical propagation of the packet can be carried out with good precision, by computing the corresponding correlation function $C_{\mathrm{scl}}(t)$ as a sum of contributions of the homoclinic excursions of the PO. This procedure has nevertheless some drawbacks, since, for example, the number of orbits that is necessary to include in the calculation to obtain converged results grows dramatically with time.

A different approach, that maintains an interpretation of wave mechanics based on more simple classical objects represented by POs has been presented elsewhere [6,7]. In this theory [6] all quantum information of a bounded chaotic Hamiltonian system can be obtained using a number of POs that grows only linearly with the Heisenberg time.

Another point worth considering is the importance and/or convenience of using wave functions that are ''dynamically adapted'' in this type of studies. By ''dynamically adapted'' [8] we mean structures that contain information not only about the PO, but also about the linearized dynamics around the orbit. When considered in phase space, these structures appear not only localized over the PO, but are also spread over the corresponding manifolds.

The construction of functions of this kind can be carried out using different approaches. In Ref. [9] the necessary information is obtained by Fourier transforming the short-time exact-quantum dynamics, so that wave functions averaged over the PO path are obtained. Kaplan and Heller [10] used a sum of coherent Gaussian wave packets centered along the PO to obtain the desired function. Finally, Vergini and Carlo [11] constructed semiclassically resonances along POs with minimum energy dispersion.

In spite of the differences existing among these functions, they are all suitable to efficiently investigate the quantum manifestations of the classical phase-space complexity in classically chaotic systems.

The purpose of this paper is threefold. First, we focus on the analysis of the topological characteristics (i.e., distribution of quantum probability) in phase space of this type of wave functions highly localized on an unstable PO. Second, special attention will be paid to the relationship existing between the quantum dynamics of this function and that of other classical POs of the system located in their vicinity, in order to explore the existence of dynamical connections and active interplay between them. Finally, another interesting aspect of these functions is their revivals, that take place in some cases for a surprisingly large number of cycles without showing any visible sign of dispersion [12]. This fact, which is particularly surprising in view of the highly chaotic character of the problem that will be considered, is due to the special dynamical properties of these functions. Summarizing, it should be stressed that the most important result of our work is that, proceeding in this way, only a few short POs

are necessary to adequately explain the quantum dynamics of this type of systems.

For our study we will use localized functions as defined in Ref. [9], applying them to the study of the dynamics in the Bunimovich stadium billiard [13], a system that is known to behave ergodically from the classical point of view.

The organization of the paper is as follows. In Sec. II we describe in detail how the method of Ref. [9] can be used to construct the desired wave functions, highly localized on a given unstable PO and their associated manifolds. Numerical results concerning the topological characteristics, both in configuration and phase space, of these functions and the corresponding time evolution will be presented and analyzed in Secs. III and IV, respectively. Finally, the main conclusions derived from our work are presented in Sec. V.

II. CONSTRUCTING LOCALIZED WAVE FUNCTIONS

In this section we briefly describe the method [9] that will be used to construct states initially located on a given PO and the corresponding manifolds. The procedure has been previously applied to the analysis of the scarring effect of unstable POs in chaotic systems [14], as well as to the study of the quantum dynamics that takes place beyond the first recurrence of the corresponding motion [7]. As it will be shown, these initial states can be used as an important tool to disentangle the complexity of the full quantum dynamics taking place in the area of influence of a given PO, making use of the associated classical mechanics as a guide in the process.

Initially, the method considers a wave function, $|\phi(0)\rangle$, well localized in phase space in the vicinity of a given PO. The corresponding time evolution can be followed by means of the associated autocorrelation function,

$$C(t)=\langle\phi(0)|\phi(t)\rangle=\langle\phi(0)|e^{-i\hat{H}t}|\phi(0)\rangle. \tag{1}$$

Recurrences in $C(t)$ are known to determine the low-resolution structure of the corresponding spectra [4],

$$I_T(E)=\frac{1}{2\pi}\int_{-\infty}^{\infty}dt\, W_T(t)C(t)e^{iEt}, \tag{2}$$

and are the origin of the scarring effect, as first discussed in [3]. $W_T(t)$ is a window function to take into account possible different resolutions in $I_T(E)$.

A widely spread choice for $|\phi(0)\rangle$ is a minimun uncertainty harmonic oscillator coherent state ($\hbar$ is set equal to 1 throughout this paper)

$$G_{\mathbf{r}^0,\mathbf{p}^0}(\mathbf{r})=\prod_j\left(\frac{1}{\pi\sigma_j^2}\right)^{1/4}\exp\left[\frac{-(r_j-r_j^0)^2}{2\sigma_j^2}\right]\times\exp[iP_j^0(r_j-r_j^0)], \tag{3}$$

where $(\mathbf{r}^0,\mathbf{P}^0)$ represents the coordinates and conjugate momenta of a suitable phase space point along the selected PO.

For bounded systems, the evolution of this packet can be followed quite conveniently by projection on a complete set of eigenfunctions $|n\rangle$ of the Hamiltonian $\hat{H}$,

$$|\phi(t)\rangle=e^{-i\hat{H}t}|\phi(0)\rangle=\sum_n|n\rangle\langle n|\phi(0)\rangle e^{-iE_nt}, \tag{4}$$

where $\{E_n\}$ is the corresponding set of eigenvalues. In our case the billiard eigenstates have been computed using the scaling method [15].

Regarding the smoothing function $W_T(t)$ one has many choices; i.e., ''hat,'' exponential or Gaussian functions, which render $\sin(x)/x$, Lorentzian or Gaussian-type line envelopes, respectively. In our case we use the Gaussian decay

$$W_T(t)=\frac{e^{-t^2/2T^2}}{T}, \tag{5}$$

for which the spectrum takes the form

$$I_T(E)=\frac{1}{(2\pi)^{1/2}}\sum_n|\langle n|\phi(0)\rangle|^2\exp[-T^2(E-E_n)^2/2]. \tag{6}$$

The center of the initial wave packet defined in Eq. (3) will follow for some time the classical PO on which it was launched, with the dispersion rate evolving according to the Lyapunov exponent of the orbit [4].

In a second step [9], a wave function highly scarred by the PO can be constructed very efficiently by considering the average of $|\phi(t)\rangle$ along the dynamics generated by the PO during a given amount of time, usually taken of the order of the PO period. Let us remark the importance of this last requirement, since if the packet is allowed to evolve for a very long time, so that due to the chaotic character of the dynamics it has the opportunity to sample all the available phase space, just the (complicated) eigenfunctions of the system will be obtained. The corresponding expression for the localized wave function corresponding to an energy E_0 (usually taken as the center of one of the bands appearing in the low-resolution spectrum generated by $|\phi(0)\rangle$) reads as follows:

$$|\psi^{E_0}\rangle=\frac{1}{2\pi}\int_{-\infty}^{\infty}dt\, e^{iE_0t}W_T(t)|\phi(t)\rangle=\frac{1}{(2\pi)^{1/2}}\sum_n|n\rangle\langle n|\phi(0)\rangle\exp[-T^2(E_0-E_n)^2/2]. \tag{7}$$

Phase-space representations for the wave functions described in this section can be constructed in a number of different ways. In this paper we will follow the procedure described in Ref. [16], which relies on the use of normal derivatives of the wave functions evaluated at the boundary of the billiard. On this boundary, Birkhoff coordinates [17] (q,p) are used to define both classical and quantal Poincaré surfaces of section such that q is the arc-length coordinate, and $p=\mathbf{p}\cdot\hat{\mathbf{t}}/|\mathbf{p}|$ is the fraction of tangential momentum. The coherent states necessary to construct this representation (Husimi functions [18]) are then defined as

$$G_{q^0p^0}(q)=\left(\frac{1}{\pi\sigma^2}\right)^{1/4}\exp\left[-\frac{1}{2\sigma^2}(q-q^0)^2\right]$$
$$\times\exp[ip^0(q-q^0)]. \quad (8)$$

This expression corresponds to a boundary wave packet at point (q^0,p^0) in the surface of section; representing a bounce off a given boundary point with a specific tangential momentum. Then, for a wave function with normal derivative on the boundary $\psi(q)$ (extended periodically to the real line), the corresponding Husimi function is given by

$$H(q^0,p^0)=|\langle G_{q^0p^0}|\psi\rangle|^2. \quad (9)$$

III. TOPOLOGICAL CHARACTERISTICS OF THE LOCALIZED WAVE FUNCTIONS

The system that we have chosen to study is a particle of mass 1/2 moving in a desymmetrized stadium billiard with Newman boundary conditions on the symmetry axes (only even-even parity wave functions will then be considered). The radius r is taken equal to unity and the enclosed area is $1+\pi/4$. This system is known to exhibit a great degree of chaoticity, both from the classical and quantal points of view.

In this case, and due to the symmetry of the problem, symmetry adapted initial wave functions should be used; the corresponding expression being given by

$$\langle x,y|\phi(0)\rangle=G_{x^0,y^0,P_x^0,P_y^0}+G_{-x^0,y^0,-P_x^0,P_y^0}+G_{x^0,-y^0,P_x^0,-P_y^0}$$
$$+G_{-x^0,-y^0,-P_x^0,-P_y^0}+\text{c.c.} \quad (10)$$

is obtained by imposing Newman boundary condition at the symmetry axes.

We consider the dynamics dominated by the horizontal PO, running along the x axis with $y=0$. Accordingly, we use for our study a symmetry-adapted Gaussian wave packet [Eq. (9)] with centers defined by the phase-space point $(x^0,y^0,P_x^0,P_y^0)=(1,0,k,0)$ and width $\sigma_x=\sigma_y=1.603/k^{1/2}$, where k is the usual wave number. The corresponding autocorrelation function for a packet with an energy at the center of $E=3600$, for which the period of the horizontal PO is equal to $T_0=1/30$, is shown in Fig. 1. As can be seen, two main peaks exist at $t\simeq 0.016$ and 0.033, respectively, the first one being substantially lower than the second. After that, the correlation function becomes very complicated. The relative intensity of the two peaks can be easily explained if one takes into account that the initial coherent state that we are using is the sum of two packets, launched with opposite values of the momentum. The two packets first separate, one being scattered by the vertical axis and the other by the circular hard wall of the billiard, so that when they first return to the initial point, at a time roughly equal to $T_0/2$, they have picked up different phases. This gives rise to the first (small) recurrence peak in $|C(t)|$. Afterwards, the two components continue moving, colliding with the circular and vertical walls, respectively. In this way, when some time later, at $t\simeq T_0$, they return again close to the initial point, both arrive with approximately the same collisional phase, this giving rise to the second, more pronounced peak in the autocorrelation function.

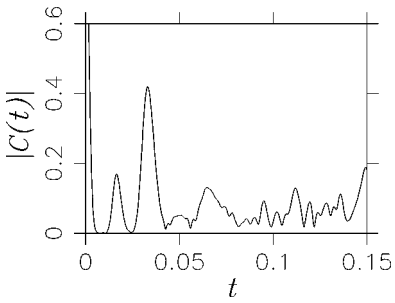

FIG. 1. Modulus of the autocorrelation function corresponding to a symmetrized wave packet [Eq. (9)] initially centered on the horizontal periodic orbit of the desymmetrized stadium billiard with Newman boundary conditions on the axes at an energy $E=3600$. The radius is taken equal to 1, the enclosed area $1+\pi/4$, and the mass of the particle 1/2.

Let us consider next the localization of the wave functions obtained with the method described in the previous section [see Eq. (7)] for different values of the smoothing time. We choose $T=0.01$, 0.03, 0.06, and 0.1, in order to cover a range of values smaller and greater than T_0. The results are shown in Fig. 2, where we present the corresponding squared wave functions, Husimi based quantum sufaces of sections, and the associated portions of the spectra generated from $|\phi(0)\rangle$. Three comments are in order.

In the first place, the wave functions in configuration space (top tier) appear localized along the PO, presenting a number of nodes m in agrement with the value obtained from the Bohr-Sommerfeld quantization condition

$$k=\frac{2\pi}{L}\left(m+\frac{\nu}{4}\right) \quad (11)$$

when applied to the spectral peaks (bottom tier). For the horizontal PO, $L=4$ and the Maslov index $\nu=3$.

In the second place, and much more importantly, in the localized wave functions it is clearly observable the distortion in the structure induced by the self-focal point. A discussion of this effect can be found in Ref. [4]. This is a very important point, and is a consequence of the fact that these functions have been defined in such a way—averaging over the motion along the orbit—that they are not only located in the right position of configuration space, but contain also information on the dynamics of the system in the vicinity of the PO. This is more clearly seen when examining the phase-space picture of these functions, i.e., middle tier of Fig. 2. There, it is observed that the probability density do not just localize over the fixed point corresponding to the scarring orbit, but it is also spread significantly along their manifolds.

Finally, this structure over the manifolds changes as the value of T is increased, giving the original packet the opportunity to explore more and more of the dynamics induced by the PO. Indeed, we see in Fig. 2 that for $T=0.01$, well before the first peak in $|C(t)|$, the quantum surface of section appear essentially localized on the fixed phase point corre-

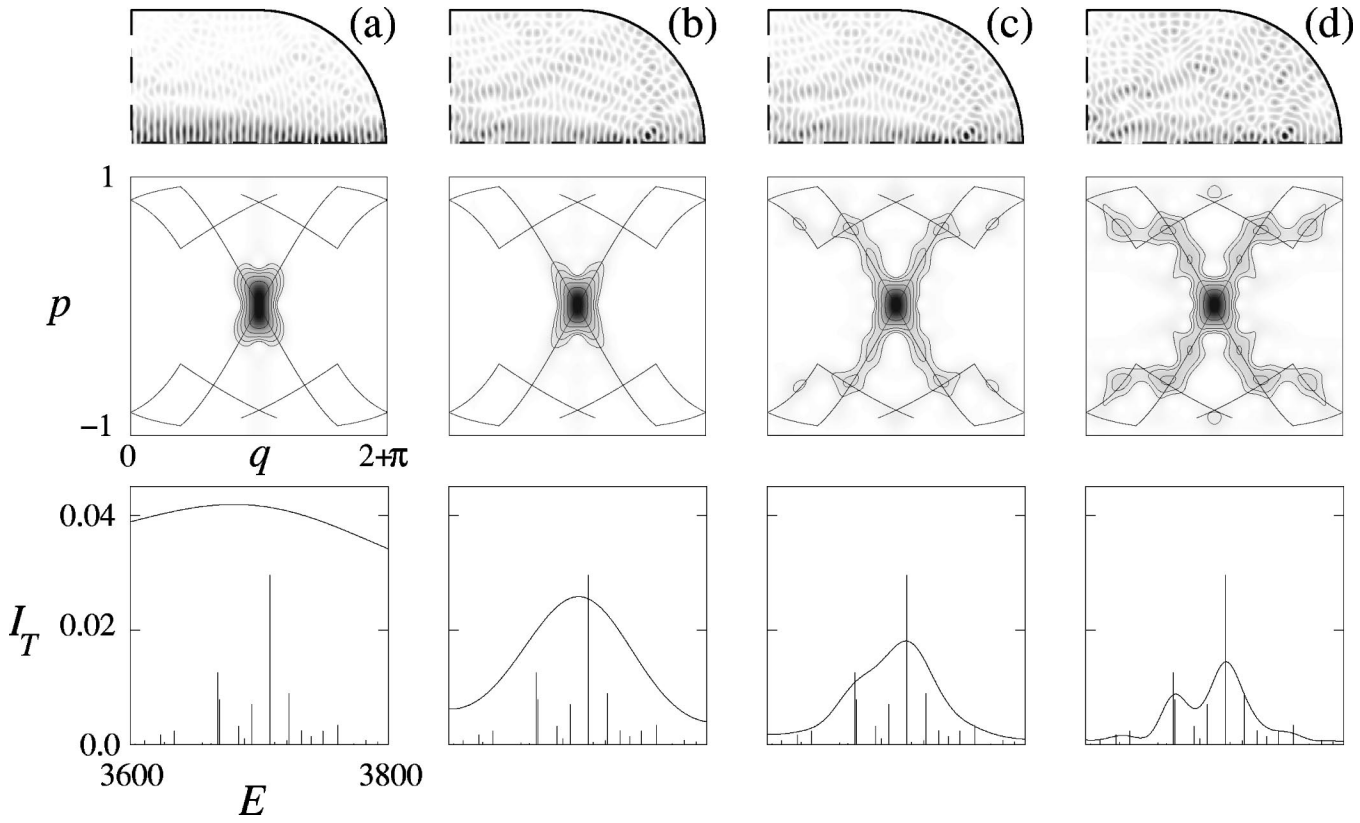

FIG. 2. (Top) Localized (squared) wave functions calculated using Eq. (7), (middle) Husimi based quantum Poincaré surface of section, and (bottom) spectra (I_∞ as a stick spectrum and I_T in solid line) for different values of the smoothing time, T: (a) 0.01, (b) 0.03, (c) 0.06, and (c) 0.1 at $E_0=3700$, corresponding to the autocorrelation function of Fig. 1. The invariant manifolds of the horizontal periodic orbit have also been drawn superimposed in the middle pannel.

sponding to the horizontal PO, with just some probability sticking out of this region along the manifolds (also plotted in the figure). For $T=0.03$ this latter effect is more pronounced, and the pattern along the linearized part of the stable and unstable manifolds is fully developed. At the same time, the corresponding low-resolution spectral envelopes $I_T(E)$ (continuous line in the bottom tier) define, with increasing precision, the clump of eigenstates contributing to this scar [9]. Past this time, i.e., for $T=0.06$, well beyond the first (true) recurrence of the horizontal PO, the original packet has had the opportunity to enter into the truly nonlinear part of the periodic trajectory, exploring regions of phase space far apart from the fixed point, where the dynamical flux gets more complicated. However, we see that the averaged wave function is well confined on the manifolds, even following the sharp kinks that they present. This process continues for $T=0.1$, value at which the localized wave function appears covering practically all these invariant structures of phase space. In this case the resolution in the spectra is higher, and the corresponding spectral envelope define several bands, four in our case. These higher-resolution bands [7] correspond to the interaction with other POs of longer periods, as will be discussed in the next section. The signatures of these longer POs are seen in the configuration space plots.

Another aspect of this problem that is worth considering is how the process described above is affected when the transition to the semiclassical limit is considered. For this purpose we have repeated the previous calculations, launching the packet from the same point as before but with different values of the energy. The results are shown in Fig. 3. In it we present the localized wave functions, Husimi based quantum Poincaré surfaces of section, and spectra for $E_0=400$ and $T=0.1$ [column (a)], and also for $E_0=40267$ and $T=0.01$ [column (b)]. These values of the smoothing times correspond to the periods of the horizontal PO at the selected energies, so that these are compared to those in Fig. 2(b). As can be seen, the structure exhibited by these functions is essentially the same, if one takes into account the fact that all length features scale as $k^{-1/2}$. This scaling is the origin of the better definition of the focalization effect existing in the configuration-space wave functions at higher energies.

Using Gutzwiller trace formulas, similar smoothed wave function has recently been calculated [19], also showing that the invariant hyperbolic classical structure is contained in quantum mechanics. In this case no dynamical information was used, with the result that many more (of the order of 10 000) states were needed in the summation in order to get the same kind of localization that we are showing in this paper.

IV. DYNAMICS OF THE LOCALIZED WAVE FUNCTIONS

In this section we investigate the dynamics of the localized wave functions described in the previous section, with

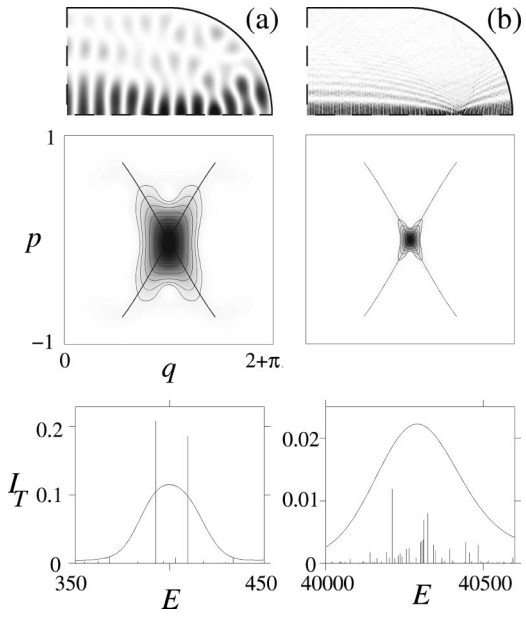

FIG. 3. (Top) Localized (squared) wave functions calculated using Eq. (7), (middle) Husimi based quantum Poincaré surface of section, and (bottom) spectra (I_∞ as a stick spectrum and I_T in solid line) for: (a) $E_0=400$ and $T=0.1$, and (b) $E_0=40\,267$ and $T=0.01$. The invariant manifolds of the horizontal periodic orbit have also been drawn superimposed in the middle pannel.

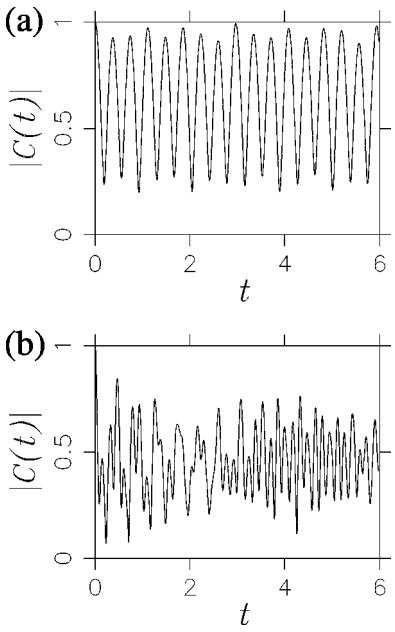

FIG. 4. Modulus of the autocorrelation function corresponding to localized wave functions calculated for: (a) $E_0=400$ and $T=0.1$, and (b) $E_0=3700$ and $T=0.03$.

the purpose of disentangling the complexity of the quantum dynamics in the problem that we are considering. As stated in the Introduction, our aim is to provide an explanation of the quantum dynamics of highly chaotic systems in terms of classical invariant structures.

In Fig. 4 we present the autocorrelation function calculated using the (nonstationary) localized wave functions [Eq. (7)] of Fig. 3(a) and Fig. 2(b). The results of part (a), corresponding to $E_0=400$ and $T=0.1$, show a series of recurrences at time intervals approximately equal to 0.38. In each of them, practically all the initial probability is recovered, and the process shows no evidence of dispersion up to the times considered in our calculations. This phenomenon has already been discussed in Ref. [12], where Gaussian wave packets ''stretched'' along the horizontal PO were used, and necessary conditions for the existence of revivals were given. As indicated before, in our case we use initial functions that

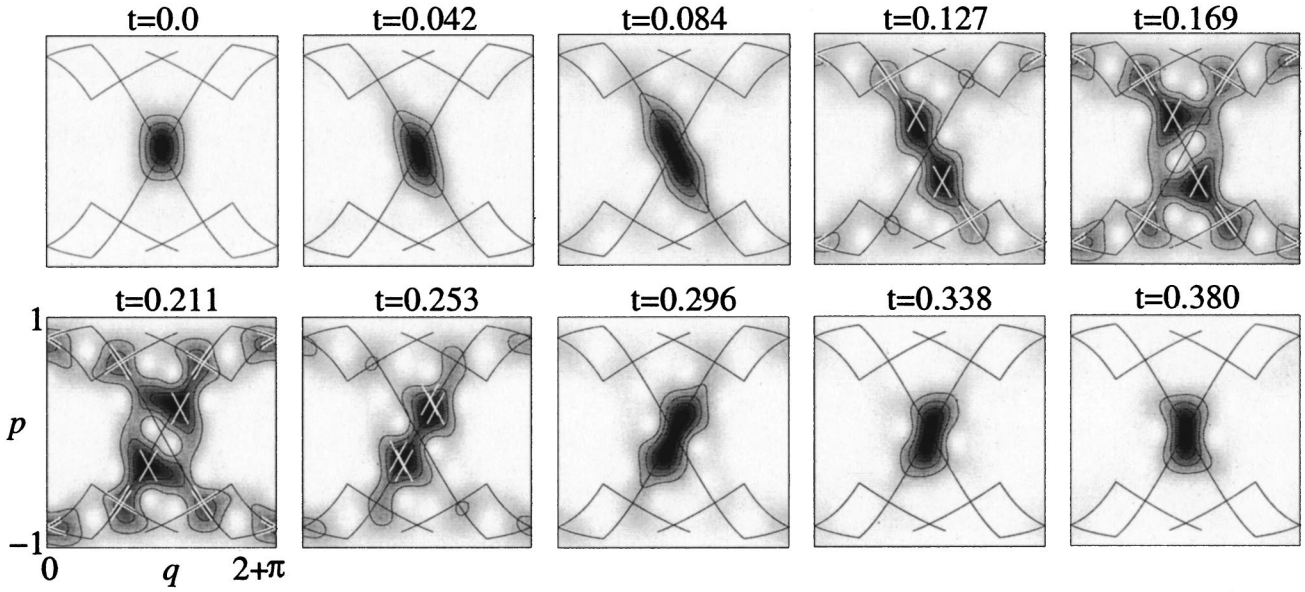

FIG. 5. Snapshots of the dynamical evolution in phase space of the localized wave function corresponding to Fig. 3(a). The manifolds of the horizontal orbit are plotted in solid line. The linearized manifolds of the orbits (1), (2), (3) and (4) of Fig. 6 are included in white lines (in the case that the Husimi function is localized on them).

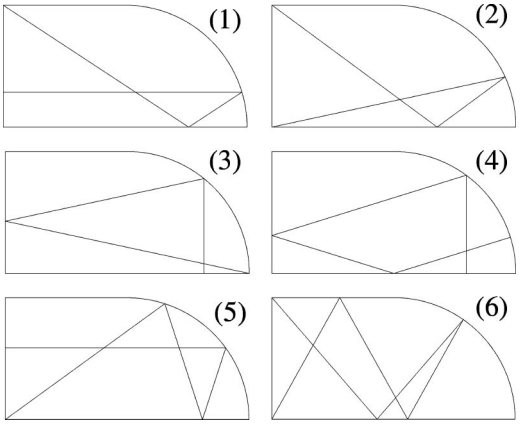

FIG. 6. Some periodic orbits of the desymmetrized stadium billiard related to the horizontal one. See text for details.

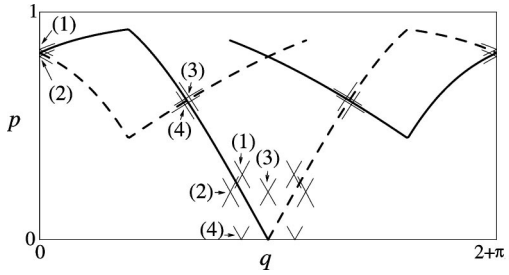

FIG. 7. Fixed points and associated manifolds of some periodic orbits in Fig. 6. The unstable (thick full line) and stable (thick dashed line) manifolds of the horizontal periodic orbit are also represented.

are better adapted to the dynamics of the orbit, thus showing an improved revival behavior. In this respect, it is important to note that, opposed to which it was found in [12], our functions show revivals, in this wavelength regime, for an ample range of energy values and also for other POs.

From the quantum-mechanical point of view these recurrences are easy to interpret, since they are the result of the beating frequency originated from the two (almost exclusive) eigenstate contribution to the initial packet (see spectrum in the bottom part of Fig. 3). On the other hand, at the classical level, the phenomenon is more difficult to understand. To further investigate these recurrences from this point of view, we show in Fig. 5 a series of snapshots in phase space covering the period of time elapsed up to the first recurrence of $|\psi^{E_0}\rangle$. Notice that due to the symmetry of the figure we have only plotted one half of the complete phase space of the billiard. To help interpreting this figure, the position of the fixed points and associated manifolds, corresponding to some short POs related to the horizontal one, have also been included. These orbits are presented in Fig. 6. For the sake of clarity, the labeling of the POs was not included in Fig. 5, but it can be found in Fig. 7.

In the first three images of Fig. 5 we see how the original probability density distribution elongates, stretching along the unstable manifolds of the horizontal PO and contracting along the stable ones. Afterwards, the process continues, populating the regions around the fixed points corresponding to orbits (3),(4) and (1),(2) [20], so that at $t=0.127-0.169$ a noticeable accumulation of probability around these points has taken place. Notice also the effect of the flux along the stable manifolds of these POs, which at $t=0.127$ is narrowing the elongated shape of the distribution along some specific lines, and at $t=0.169$ has split the packet in several pieces. At $t=0.211$ this process reaches its maximum, and the probability remaining in the initial region is practically zero. After this point, the evolution continues in a similar way with the probability returning gradually to the vicinity

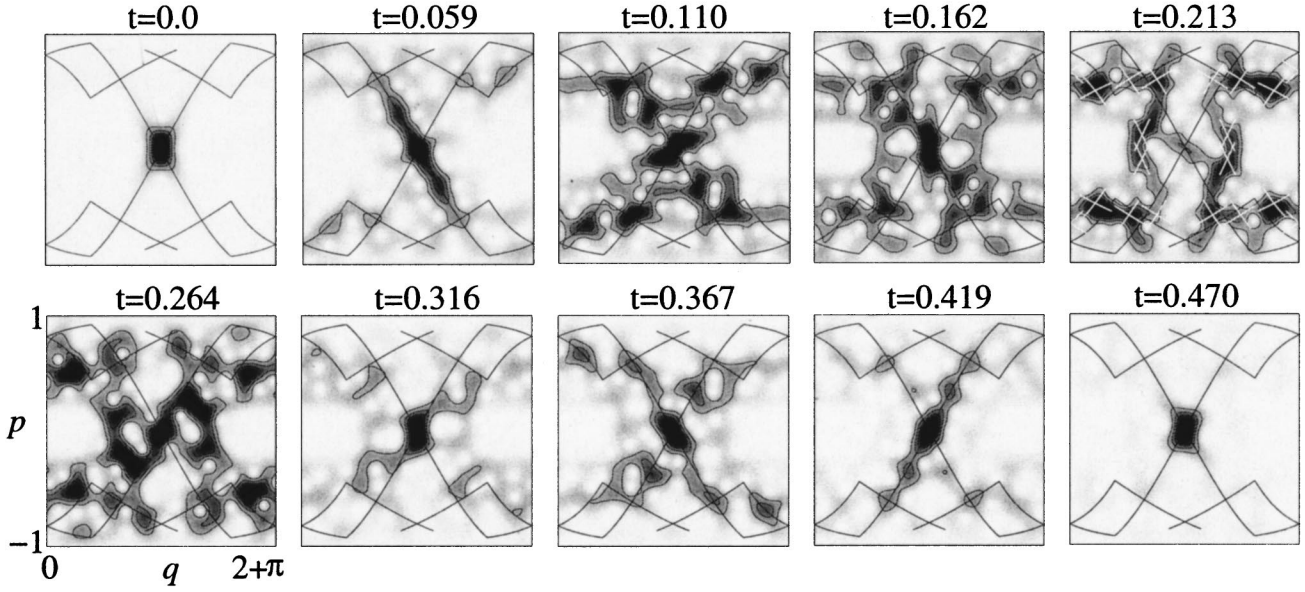

FIG. 8. Snapshots of the dynamical evolution in phase space of the localized wave function corresponding to Fig. 2(b). The manifolds of the horizontal orbit are plotted in solid line. The linearized manifolds of the orbits (5) and (6) of Fig. 6 are included in white lines at $t=0.213$.

of the initial point, although obviously this time following a path going along the stable manifolds. This second half of the dynamics takes place following the same series of intermediate steps.

In Fig. 4(b) the autocorrelation function for the initial state of Fig. 2(b) is shown. In this case the recurrence pattern is much more complex, but it is nevertheless noticeable that the existence of a fairly good number of recurrences in which the overlap with the initial distribution is greater than 50%. The difference with the example presented in Fig. 4(a) is clear. In this case, the initial wave function is formed by a substantially greater number of contributions [see the associated spectrum at the bottom of Fig. 2(b)], and then the probability that all of them get in phase is much smaller. The corresponding evolution in phase space is presented, up to the first big recurrence at $t \simeq 0.47$, in Fig. 8. At this higher energy we see that the mechanism for the dispersion of the probability density is practically the same, although there exist certain differences worth commenting. In the first place, the time scale for the dispersion is obviously faster, i.e., compare the extent of the evolution in the first snapshot at $t=0.059$ with the third one at $t=0.127$ of Fig. 5. In the second place, the probability distribution appears in this case much more localized on the participating invariant classical structures for all values of time considered. Finally, at certain values of t, the probability shows peaks that localize on new POs, not important for the dynamical evolution at $E_0=400$ shown in Fig. 5. For example, at $t=0.213$ the probability density localizes on orbits (5) and (6) of Fig. 6. This effect is not unexpected, since it is reasonable to admit that as we increase the energy, going towards the semiclassical limit, more POs are necessary to explain the quantum dynamics of our system, as discussed in Ref. [6].

V. SUMMARY AND CONCLUSIONS

The introduction of Gutzwiller's trace formula [2] provided a method to understand the quantum mechanics of classically chaotic Hamiltonian systems in terms of POs. Its main drawback is the exponential growth in the number of orbits involved as the Heisenberg time T_H increases, and many efforts have been devoted to the development of resummation techniques that improve its convergence.

Our work considers an alternative approach, initiated with Refs. [6,7], based on the use of special functions well localized on a few POs and its manifolds, the number of which grows only linearly with T_H. To construct these localized functions we have used the method described in Ref. [9], based on the dynamics of a coherent wave packet averaged along a given PO and its neighborhood.

In this paper we have studied in detail some important characteristics and properties of these nonstationary-scarred functions in the case of the horizontal PO in the desymmetrized Bunimovich stadium billiard, a paradigmatic example of chaos. In particular, we have considered how the localization properties, both in configuration and phase space, of these functions calculated at energies E_0 close to the Bohr-Sommerfeld quantization conditions vary with the averaging time T. Our results show that the probability density in phase space extends along the manifolds of the scarring PO, even when the associated dynamics have left the linear regime. In the second place, the transition to the semiclassical limit has also been investigated by simultaneously changing E_0 and T. As it takes place, all length features get better defined, for example, the focal points corresponding to the hyperbolic structure around the fixed point. Finally, we have also studied the dynamics of these nonstationary wave functions. When the corresponding probability density in phase space is followed a dispersion along the manifolds is observed. In this process a building up of probability peaks takes place on a few POs related to the original one (the horizontal PO in our case). The recurrences in the corresponding autocorrelation function can be very important, and we have even shown one example in which they are particularly pronounced.

To conclude, we think that this work provides valuable information that can help in the disentanglement of the quantum mechanics of very chaotic Hamiltonian systems in terms of simple classical structures.

ACKNOWLEDGMENTS

This work was partially supported by PICT97 03-00050-01015, SECYT-ECOS (Argentina), and DGES (Spain) Under Contracts Nos. PB96-76, PB98-115, and BMF2000-437. D.A.W. gratefully acknowledges support from CONICET (Argentina) and AECI (Spain).

[1] M.C. Gutzwiller, Am. J. Phys. **66**, 304 (1997); H.-J. Stöckmann, *Quantum Chaos: An Introduction* (Cambridge University Press, Cambridge, England, 1999).

[2] M.C. Gutzwiller, *Chaos in Classical and Quantum Mechanics* (Springer-Verlag, New York, 1990); L.E. Reichl, *The Transition to Chaos in Conservative System: Quantum Manifestations* (Springer-Verlag, New York, 1992).

[3] E.J. Heller, Phys. Rev. Lett. **53**, 1515 (1984).

[4] E.J. Heller, in *Chaos and Quantum Physics*, edited by M.-J. Giannoni, A. Voros, and J. Zinn-Justin (North-Holland, Amsterdam, 1991).

[5] S. Tomsovic and E.J. Heller, Phys. Rev. Lett. **67**, 664 (1991); Phys. Rev. E **47**, 282 (1993).

[6] E. Vergini, J. Phys. A **33**, 4709 (2000); E. Vergini and G. Carlo, *ibid.* **33**, 4717 (2000).

[7] D.A. Wisniacki, F. Borondo, E. Vergini, and R.M. Benito, Phys. Rev. E **62**, R7583 (2000).

[8] W. Schweizer, W. Jans, and T. Uzer, Phys. Rev. A **58**, 1382 (1998).

[9] G.G. de Polavieja, F. Borondo, and R.M. Benito, Phys. Rev. Lett. **73**, 1613 (1994).

[10] L. Kaplan and E.J. Heller, Ann. Phys. (N.Y.) **264**, 171 (1998);

L. Kaplan, Nonlinearity **12**, R1 (1999).
[11] E. Vergini and G. Carlo, J. Phys. A (to be published).
[12] S. Tomsovic and J.H. Lefebvre, Phys. Rev. Lett. **79**, 3629 (1997).
[13] L.A. Bunimovich, Commun. Math. Phys. **65**, 295 (1079).
[14] F. Borondo and R.M. Benito, in *Wave Packets in Physics and Chemistry*, edited by J. Yeazell and T. Uzer (Wiley, New York, 2000).
[15] E. Vergini and M. Saraceno, Phys. Rev. E **52**, 2204 (1995).
[16] J.-M. Tualle and A. Voros, Chaos, Solitons Fractals **5**, 1085 (1995).
[17] V.I. Arnold and A. Avez, *Ergodic Problems of Classical Mechanics* (Addison-Wesley, Reading, MA, 1989).
[18] K. Husimi, Proc. Phys. Math. Soc. Jpn. **22**, 264 (1940).
[19] D.A. Wisniacki and E. Vergini, Phys. Rev. E **62**, R4513 (2000).
[20] Notice that the first homoclinic intersection of the stable and unstable manifolds of the horizontal PO also takes place in this region.